JACS
JOURNAL OF THE AMERICAN CHEMICAL SOCIETY

Communication

pubs.acs.org/JACS

Reproducible Synthesis and High Porosity of mer-$Zn(Im)_2$ (ZIF-10): Exploitation of an Apparent Double-Eight Ring Template

Joseph R. Ramirez, Haiyang Yang, Christopher M. Kane, Amanda N. Ley, and K. Travis Holman*

Department of Chemistry, Georgetown University (GU), Washington, D.C. 20057, United States

Supporting Information

ABSTRACT: Reproducible synthesis of the elusive merlinoite (**mer**) topology of zinc imidazolate (**mer**-$Zn(Im)_2$, or ZIF-10) has been achieved by employing a simple macrocyclic solute—**MeMeCH$_2$**—as a kinetic template. The corresponding phase-pure material, **mer-MeMeCH$_2$**@$Zn_{16}(Im)_{32}$, is confirmed to be porous and exhibits one of the highest experimental surface areas (1893 m^2/g, BET) yet reported for any ZIF. The X-ray single crystal structure of **mer-MeMeCH$_2$**@$Zn_{16}(Im)_{32}$·*x*solvent reveals the role of the macrocyle as an 8-fold hydrogen bond acceptor in templating the requisite double-eight rings (*d8r*) of the **mer** framework.

Zeolitic imidazolate frameworks (ZIFs)[1,2] are a class of (typically) porous zeolite-like metal−organic frameworks (ZMOFs)[3,4] that are widely studied due to their diverse structures, high chemical and thermal stabilities, and myriad of potential applications that stem from their high surface areas and pore volumes.[5] In terms of structural diversity, much interest in ZIFs is related to their being expanded analogues of the technologically essential aluminosilicate zeolites, attributable to their construction from simple tetrahedral metal centers (e.g., M = Zn^{2+}, Co^{2+}, and Cd^{2+}) and bent imidazolate (Im^-)—or functionalized imidazolate (RIm^-)—bridging ligands. Thus, akin to zeolites, it is understood that a large number of framework topologies are in principle possible for any given $M(RIm)_2$ composition. For example, the most chemically trivial of compositions, $Zn(Im)_2$, is currently known to exist in 12 different framework topologies[6]—**zni**,[7] **cag** (ZIF-4),[8] **crb** (BCT, ZIF-1,2),[8] **coi**,[2b] **gis** (ZIF-6),[1a] **dft** (ZIF-3),[8] **nog**,[8] **zec**,[8] **neb**,[9] **sod**,[10] **mer** (ZIF-10, Figure 1)[1a,b] and a form exhibiting ten-membered rings (**10mr**).[11] Despite the structural diversity of $Zn(Im)_2$, and the demonstration of high porosity in many other ZIF compositions—e.g., **sod**-$Zn(MeIm)_2$, ZIF-8, ≤1750 m^2/g;[12] **gme**-$Zn(Im)_{1.13}(NO_2Im)_{0.87}$, ZIF-70, 1730 m^2/g;[13] **rho**-$Cd(EtIm)_2$, CdIF-4, 1630 m^2/g,[14] etc.—the $Zn(Im)_2$ frameworks have not been shown to sustain high porosity.[15] Several of the $Zn(Im)_2$ topologies are probably too dense to be useful for sorption applications, and the more open frameworks are either susceptible to collapse upon activation (e.g., **dft**-$Zn(Im)_2$), or appear to only be available in single crystal quantities.[10] Thus, only **sod**-$Zn(Im)_{1.7}(MeIm)_{0.3}$, prepared by (incomplete) ligand exchange on **sod**-$Zn(MeIm)_2$ (ZIF-8),[10] exhibits high surface area ($830\ m^2\ g^{-1}$), but the value falls well below the theoretical limit for the **sod** framework.

Unfortunately, reproducible synthetic procedures that yield phase-pure material are lacking for many potentially useful ZIFs, including some key $Zn(Im)_2$ structures. For instance, the merlinoite (**mer**) topology of $Zn(Im)_2$, first reported by Yaghi and co-workers,[1a,b] has been particularly elusive. To date, it has only been reported as solvated individual crystals isolated from reaction of zinc nitrate and imidazole in dimethylformamide (DMF).[1a,b] Attempts to reproduce the published syntheses have not been successful (see ESI). Thus, no yield, experimental PXRD pattern, or gas sorption isotherm has yet been reported for **mer**-$Zn(Im)_2$. This is despite the fact that **mer**-$Zn(Im)_2$ may be a material of importance: it has the highest porosity ($\varepsilon \approx 61\%$) of any known $Zn(Im)_2$ topology and one of the lowest framework densities of any ZIF (0.75 g/cm^3). Moreover, the sorption properties of **mer**-$Zn(Im)_2$ have been of interest to theorists, especially in the context of gas separations.[16]

Unfortunately, it remains unclear whether ZIFs of the **mer** topology are capable of sustaining high porosity upon activation. Only two other **mer** topology ZIFs have been reported in phase-pure form (PXRD patterns)—solvated forms of **mer**-$Zn(MeIm)_{1.5}(Im)_{0.5}$·*x*solvent (ZIF-60)[1b] and **mer**-$Cd(Im)_2$·*x*solvent (CdIF-2)[14a]—and neither has yet been shown to be porous. In fact, **mer**-$Cd(Im)_2$ was found to collapse upon activation, despite the fact that **rho**-$Cd(RIm)_2$ frameworks exhibit high

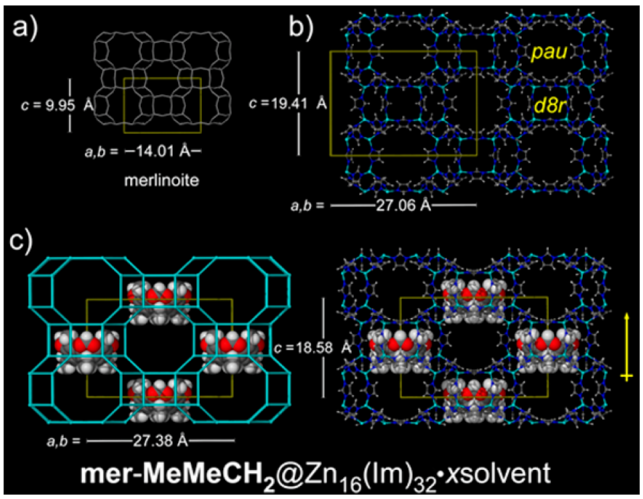

Figure 1. Comparative depictions of the framework structures of (a) the zeolite mineral merlinoite, (b) *I*4/*mmm* **mer**-$Zn(Im)_2$·*x*solvent (ZIF-10),[1] (c) polar, *I*4*mm* **mer-MeMeCH$_2$**@$Zn_{16}(Im)_{32}$·*x*DMF (disorder omitted). The **MeMeCH$_2$** macrocyles (spacefill) reside in the *d8r*s of the framework.

Received: June 25, 2016
Published: September 7, 2016

DOI: 10.1021/jacs.6b06375
J. Am. Chem. Soc. 2016, 138, 12017−12020

porosities.[14] We report here a reproducible synthesis of phase-pure **mer**-$Zn(Im)_2$ (ZIF-10), in the form of **mer-MeMeCH$_2$@**$Zn_{16}(Im)_{32}$ (or **mer-MeMeCH$_2$@**ZIF-10) achieved by introducing a readily available macrocyclic solute, **MeMeCH$_2$** (Scheme 1),

Scheme 1. Exemplary Cavitands

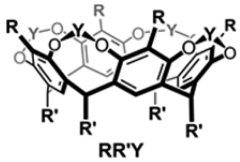

as a structural template for the requisite double-eight rings (*d8r*s) of the **mer** topology. The low temperature/pressure N_2 sorption isotherm confirms its effective activation and shows that it exhibits one of the highest experimental per-gram surface areas of any ZIF to date. The crystal structure of **mer-MeMeCH$_2$@**$Zn_{16}(Im)_{32}$·*x*solvent illustrates the role of the C_4-symmetric macrocycle in templating the C_4-symmetric *d8r*s.

Several strategies exist for the targeting of open ZMOF and ZIF framework topologies.[4] For example, akin to templation strategies employed for zeolites, the topologies of certain anionic ZMOFs have been shown to be susceptible to the organic cations during synthesis.[4] Other strategies include building block approaches whereby certain metal−ligand combinations predisposed to form requisite structural building units (SBUs) are exploited.[4,17] Being uncharged, structure-directing strategies for the simple $M(RIm)_2$ ZIFs (and MOFs, more broadly[18]) have seemingly been limited, and are not often well understood. Simple factors such as metal ion size,[14a] ligand substituents (choice of R in RIm^-,[19] or mixed ligands[13]), choice of reaction conditions (base, concentration, temperature, time), solvents,[8] or cosolvents[17] have been demonstrated to influence the topologies of ZIF products. Early on, Tian et al. demonstrated that the topologies of isolated $Zn(Im)_2$·*x*solvent crystals are highly dependent on the temperature, base, time, and solvent.[8] Importantly, the crystal structures of many $M(Im)_2$ ZIFs show that the imidazolate ligands commonly engage in C−H···acceptor hydrogen bonds with the encapsulated solvents. The topologies of ZIFs may therefore be susceptible to templation by appropriately chosen hydrogen bond acceptors. Though salts have been shown to influence the topologies of ZIFs made by mechanochemical or solventless means,[20] to our knowledge no neutral solute additives have yet been demonstrated to act as templates in ZIF syntheses.

We and others[21] have recently begun to explore the confinement of useful solute molecules within ZIFs; the large number of possible topologies suggests that ZIF frameworks may be capable of accommodating a wide range of molecules. We reasoned that Cram's ubiquitous and persistently bowl-shaped cavitands (**RR′Y**, Scheme 1)[22] may be interesting candidates for encapsulation, in the sense that (i) they introduce a well-known molecular recognition element into the pores, (ii) they may allow systematic tuning/modification of pore volume, surface area, and/or pore accessibility, (iii) they may act as structure-directing agents for larger-pore ZIFs, possibly imparting their symmetry on the ZIF structure, and/or (iv) they may, by virtue of their rigidity, support and stabilize the frameworks of large pore ZIFs with respect to collapse. Additionally, we have recently shown that many simple cavitands are porous molecular solids in their own right.[22] Some of these (e.g., **MeHSiMe$_2$**) have been shown to enclathrate/confine gases selectively within their zero-dimensional (0D) pores. Most 0D porous cavitands, however, exhibit low permeabilities. So, we sought to embed cavitands into open frameworks in order to further explore their gas recognition properties, particularly with respect to noble gas affinity.[23] Conveniently, also, the simplest cavitands are cheap (many-gram quantities), can be easily modified at the upper (**R**) and lower (**R′**) rims, and can withstand the solvothermal conditions of ZIF syntheses.

Early in the synthetic screening effort it became apparent that **MeMeCH$_2$** reproducibly induces the formation of the **mer**-$Zn(Im)_2$ framework under a variety of conditions (see ESI, methods A−C). In short, reaction of $Zn(NO_3)_2{\cdot}4H_2O$ with imidazole in DMF (or 1:1 DMF/DEF), at elevated temperatures in the presence of nearly saturated concentrations of **MeMeCH$_2$** always (according to PXRD) gave appreciable amounts of **mer** topology $Zn(Im)_2$. Single crystals (4*mm* point group) of composition **mer-MeMeCH$_2$@**$Zn_{16}(Im)_{32}$·*x*solvent (**MeMeCH$_2$@**ZIF-10) could always be identified in the reactions (Figure 1, S2). Variation of the reaction conditions resulted in the following general observations: (i) the relative amount of **MeMeCH$_2$@**ZIF-10 in the initial product mixture was seemingly proportional to the cavitand concentration, (ii) **MeMeCH$_2$@**ZIF-10 is a kinetic product, appearing as the first identifiable crystalline product and often giving way over time to **cag**-$Zn(Im)_2{\cdot}0.5$DMF (ZIF-4), once it appears (method A), in accordance with Ostwald's rule of stages, (iii) as compared to reactions that employed an 8-fold excess of Im, a stoichiometric (2:1) Im:Zn ratio considerably delayed the first appearance of **MeMeCH$_2$@**ZIF-10. Excess Im presumably accelerates the reaction by acting as a base that assists in the deprotonation of coordinated Im ligands. Lastly, control experiments, lacking **MeMeCH$_2$**, gave only ZIF-4 (Figure S4, S5) under all conditions, clearly demonstrating the structure-directing effect of the macrocycle. Unfortunately, the various conditions commonly (method A) or occasionally (method B) yielded mixtures of **MeMeCH$_2$@**ZIF-10 along with other precipitates in relative amounts ranging from a few percent (method B; unidentifiable byproducts) to sometimes more than half (method A; ZIF-4 is main impurity). Attempts to separate **MeMeCH$_2$@**ZIF-10 from the ZIF-4 and other impurities by exploiting density differences were only modestly successful (see ESI).

Ultimately, however, it was found that phase-pure **MeMeCH$_2$@**ZIF-10 could be reliably obtained (13−22%) by decreasing the ligand:metal ratio from 8:1 to 2:1 (thereby greatly lengthening the total reaction time) and seeding the reaction vials with crushed single crystals of the product that were selected from earlier preparations (method C, see ESI; Figure 2). Importantly, all of the observed peaks in the PXRD pattern (298 K) of the as-synthesized **mer-MeMeCH$_2$@**$Zn_{16}(Im)_{32}$·*x*solvent (Figure 2d) could be reliably indexed to a tetragonal unit cell (*I*4*mm*, $a = 27.177(9)$ Å, $c = 19.35(1)$ Å, $V = 14295$ Å^3, Figure S7) that is consistent with that obtained by single crystal X-ray diffraction (SCXRD) at 100 K (*I*4*mm*, $a = 27.373(3)$ Å, $c = 18.583(2)$ Å, 13923 Å^3), demonstrating the phase-purity of the sample. Interestingly, under the seeded reaction conditions, the phase-pure **mer-MeMeCH$_2$@**ZIF-10 did not appear to convert to ZIF-4 over time (30 days), presumably due to an absence of ZIF-4 seeds.

The single crystal structure of **mer-MeMeCH$_2$@**$Zn_{16}(Im)_{32}$·*x*solvent (Figure 1, S13−16) confirms the topology of the framework and reveals the remarkable structure-directing role of the **MeMeCH$_2$** template. Of course, like its MER zeolite and ZIF-10 analogues, the framework of **mer-MeMeCH$_2$@**ZIF-10 consists entirely of 8-rings and 4-rings that are arranged in two composite

DOI: 10.1021/jacs.6b06375
J. Am. Chem. Soc. 2016, 138, 12017−12020

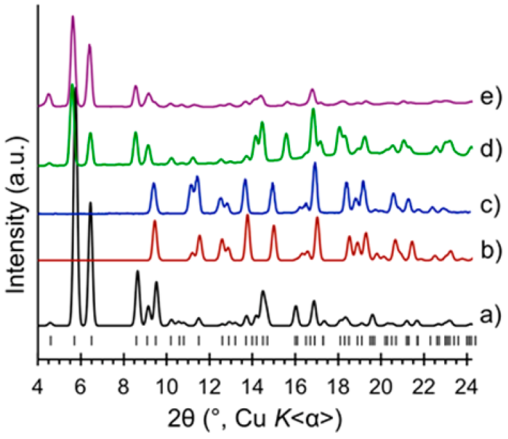

Figure 2. (a,b) Calculated PXRD patterns of **MeMeCH$_2$**@ZIF-10·*x*solvent (100 K) and **cag**-Zn(Im)$_2$·0.5DMF (ZIF-4, 100 K), respectively. The tick marks indicate the possible (*hkl*) peak positions of the former. (c–e) Experimental PXRD patterns (298 K) of (c) bulk **cag**-Zn(Im)$_2$·0.5DMF (ZIF-4) obtained in synthetic control experiments (e.g., method C) performed in the absence of **MeMeCH$_2$**, (d) as-synthesized, phase-pure **MeMeCH$_2$**@ZIF-10·*x*solvent obtained via templated synthesis (method C: **MeMeCH$_2$** and seeding), and (e) the material from pattern d, but after activation and gas sorption analysis; indexing of the pattern establishes retention of the **mer** topology.

building units (CBUs) that alternate along the *c*-axis: a double-8 ring (*d8r*) cage of 16 tetrahedral Zn^{2+} centers, and a larger Paulingite (*pau*) cage of 32 Zn^{2+} centers (Figure 1b), each connected by bridging imidazolate ligands. Although the structures of **mer**-ZIF-10 and **mer-MeMeCH$_2$**@ZIF-10 are topologically identical, a number of structural differences exist. Most notably, one molecule of **MeMeCH$_2$** appears to reside in each of the *d8r*s of the latter. ^{1}H NMR analysis of the bulk material confirms that there are ∼1.1 **MeMeCH$_2$** cavitands per *d8r*.

Importantly, each of the eight imidazolate "struts" connecting opposing 8-rings in **mer-MeMeCH$_2$**@ZIF-10 is clearly engaged in a short C–H···O hydrogen bond (C···O = 3.135(6) Å, Figure 3)

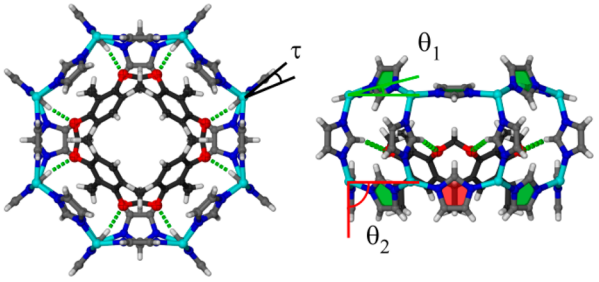

Figure 3. Illustration of the **MeMeCH$_2$** cavitand residing in the *d8r*s of **mer-MeMeCH$_2$**@ZIF-10. Structure-directing C–H···O interactions between the bridging Im$^-$ ligands and the oxygen atoms of the **MeMeCH$_2$** template are shown. The red Im$^-$ rings are those that are appear to be perturbed by the cavitand. For clarity, the mean positions of disordered Im$^-$ ligands are shown.

with one of the eight oxygen atoms of the **MeMeCH$_2$** template. The interactions involve the relatively acidic C–H groups at the 2-positions of the imidazolate ligands. Given that electron deficient azoles are known to serve as strong hydrogen bond donors,[24] it seems clear that the **MeMeCH$_2$** solute directs the formation of the **mer** topology by templating the formation of the requisite *d8r*s during crystal nucleation. The C–H···O hydrogen bonds also appear to induce subtle differences in the relative orientations of the corresponding Im$^-$ ligands in comparison to ZIF-10 (Figure S15). Moreover, as compared to their relative orientations in ZIF-10, the lower rim $CHCH_3$ moieties of the **MeMeCH$_2$** bowls (**R′**, Scheme 1) appear to force four of the Im$^-$ ligands of the closest 8-ring to turn away from the 8-ring plane (Figure 3; Im$^-$ ligands in red, $\theta_2 \gg \theta_1$). Accordingly, the typical 4/*mmm* (D_{4h}) point group symmetry of the *d8r*s is reduced to 4*mm* (C_{4v}). The relative conformations of the framework Im$^-$ ligands apparently communicate this information to adjacent *d8r*s, over a range of ∼20 Å, resulting in a polar crystal (*I*4*mm vs. I*4/*mmm* in ZIF-10). The dipole moments of the **MeMeCH$_2$** bowls in **MeMeCH$_2$**@ZIF-10 are aligned parallel with the *c*-axis, suggesting possibilities for the alignment of NLO chromophores within the polar pores of **mer-MeMeCH$_2$**@ZIF-10.[25]

Though the *d8r*s of **mer-MeMeCH$_2$**@ZIF-10 are occupied by the cavitands, the guest only modestly affects the overall pore volume of the framework. The Zn(Im)$_2$ framework occupies about 39% of the crystal volume while the **MeMeCH$_2$** cavitands occupy another 11%, leaving 50% of the crystal as solvent accessible space. The calculated density of **mer-MeMeCH$_2$**@ZIF-10 is only 0.92 g/cm^3, about the same as **sod**-Zn(MeIm)$_2$ (ZIF-8). Crystals of **mer-MeMeCH$_2$**@ZIF-10·*x*solvent were easily activated by first exchanging the included solvent with $CHCl_3$ and then heating to 80 °C under dynamic vacuum. According to ^{1}H NMR spectroscopy (Figures S8,11), **MeMeCH$_2$** does not leach from the pores during washing or activation, suggesting tight binding of the cavitand by the *d8r*s of the framework. The Type-I low temperature/pressure (77K) N_2 sorption isotherm of the activated **mer-MeMeCH$_2$**@ZIF-10 is shown in Figure 4. Clearly,

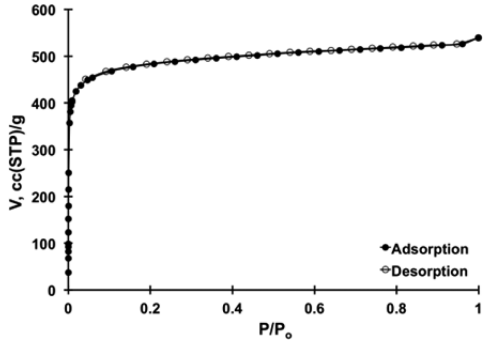

Figure 4. N_2 sorption (closed circles) and desorption (open circles) isotherms of **mer-Me,Me,CH$_2$**@ZIF-10 obtained at 77 K. BET surface area: 1893 m^2/g (1970 m^2/g Langmuir).

the cavitands do not significantly inhibit access to the pores. The data yield a BET surface area of 1893 m^2/g (Figure S10; 1970 m^2/g Langmuir) and a micropore volume of 0.74 cm^3/g (H–K method). Considering the partial filling of the pores and the extra mass introduced by the cavitand, the measured pore volume is comparable to the theoretical pore volume for empty **mer**-Zn(Im)$_2$ (0.95 cm^3/g).[16a] Postsorption SCXRD and PXRD analysis of **mer-MeMeCH$_2$**@ZIF-10, unequivocally establish that the **mer** structure is maintained upon activation (Figure 2e and S9d; see ESI). Thus, these data establish the first example of a porous MOF of the **mer** topology, and show that **mer-MeMeCH$_2$**@ZIF-10 exhibits one of the highest reported surface areas for any known ZIF. It is not yet known whether, according to the hypothesis, the **MeMeCH$_2$** cavitand serves to stabilize the **mer**-Zn(Im)$_2$ framework with respect to collapse—we remain unable to prepare **mer**-ZIF-10 that is free of cavitand. Surprisingly,

DOI: 10.1021/jacs.6b06375
J. Am. Chem. Soc. 2016, 138, 12017–12020

and unfortunately, attempts to synthesize **mer**-ZIF-10 by employing crystals of **mer-MeMeCH$_2$**@ZIF-10 as seeds in reactions that otherwise lack cavitand have so far yielded only ZIF-4 (Figure S12).

In conclusion, a reproducible synthesis of the elusive merlinoite topology of zinc imidazolate (**mer**-Zn(Im)$_2$, or ZIF-10) has been achieved by exploiting a simple macrocyclic solute, **MeMeCH$_2$**, as a kinetic template. Phase-pure **mer-MeMeCH$_2$**@ZIF-10 is easily activated and exhibits high porosity. The crystal structure of **mer-MeMeCH$_2$**@Zn$_{16}$(Im)$_{32}$·*x*solvent reveals the role of the macrocyle as a multifold hydrogen bond acceptor in templating the requisite double-eight rings (*d8r*) of the **mer** toplology. Preliminary data suggests that other **RR′CH$_2$**-type cavitands can also be incorporated into **mer**-Zn(Im)$_2$ and efforts in this direction are ongoing. It seems likely also that other novel **mer** compositions (e.g., **mer**-M(Im)$_2$ (M = Co, Cd) or **mer**-BIFs[26]) should be achievable using cavitands as templates. Though, at this time, it is unclear why the **MeMeCH$_2$** induces the formation of **mer**-Zn(Im)$_2$, instead of other default topologies that exhibit *d8r*s—such as the as-yet unknown **rho**-Zn(Im)$_2$—we expect that these may also be achievable under appropriate conditions using these *d8r* templates. More broadly, the results suggests that judiciously chosen solute additives, with appropriately positioned hydrogen bond acceptor sites, will be useful in templating, modifying the pore properties, and possibly stabilizing desirable ZIF architectures.

■ ASSOCIATED CONTENT

Supporting Information

The Supporting Information is available free of charge on the ACS Publications website at DOI: 10.1021/jacs.6b06375.

Crystallographic data in CIF format (CIF).
Syntheses, NMR spectra, crystallographic details (PDF).

■ AUTHOR INFORMATION

Corresponding Author

*kth7@georgetown.edu

Notes

The authors declare no competing financial interest.

■ ACKNOWLEDGMENTS

We thank Rahul Banerjee (CSIR-National Chemical Laboratory, India) for helpful discussions and for suggesting that we attempt to incorporate cavitands into ZIFs. We thank GU and the U.S. NSF (CHE-1337975, DMR-1610882) for support of this work. CCDC depository number 1486392 contains the single-crystal X-ray structure data for this paper.

■ REFERENCES

(1) (a) Park, K. S.; Ni, Z.; Côté, A. P.; Choi, J. Y.; Huang, R.; Uribe-Romo, F. J.; Chae, H. K.; O'Keeffe, M.; Yaghi, O. M. *Proc. Natl. Acad. Sci. U. S. A.* **2006**, *103*, 10186−10191. (b) Banerjee, R.; Phan, A.; Wang, B.; Knobler, C.; Furukawa, H.; O'Keeffe, M.; Yaghi, O. M. *Science* **2008**, *319*, 939−943. (c) Phan, A.; Doonan, C. J.; Uribe-Romo, F. J.; Knobler, C. B.; O'Keeffe, M.; Yaghi, O. M. *Acc. Chem. Res.* **2010**, *43*, 58−67.

(2) (a) Tian, Y. Q.; Cai, C. X.; Ji, Y.; You, X. Z.; Peng, S. M.; Lee, G. H. *Angew. Chem.* **2002**, *114*, 1442; *Angew. Chem., Int. Ed.* **2002**, *41*, 1384−1386. (b) Tian, Y. Q.; Cai, C. X.; Ren, X. M.; Duan, C. Y.; Xu, Y.; Gao, S.; You, X. Z. *Chem. - Eur. J.* **2003**, *9*, 5673−5685. (c) Tian, Y. Q.; Chen, Z. X.; Weng, L. H.; Guo, H. B.; Gao, S.; Zhao, D. Y. *Inorg. Chem.* **2004**, *43*, 4631−4635.

(3) (a) Keller, S. W. *Angew. Chem., Int. Ed. Engl.* **1997**, *36*, 247−248. (b) Keller, S. W.; Lopez, S. *J. Am. Chem. Soc.* **1999**, *121*, 6306−6307.

(4) (a) Liu, Y.; Kravtsov, V. C.; Larsen, R.; Eddaoudi, M. *Chem. Commun.* **2006**, 1488−1490. (b) Eddaoudi, M.; Sava, D. F.; Eubank, J. F.; Adil, K.; Guillerm, V. *Chem. Soc. Rev.* **2015**, *44*, 228−249.

(5) (a) Pimentel, B. R.; Parulkar, A.; Zhou, E.; Brunelli, N. A.; Lively, R. P. *ChemSusChem* **2014**, *7*, 3202−3240. (b) Chen, B.; Yang, Z.; Zhu, Y.; Xia, Y. *J. Mater. Chem. A* **2014**, *2*, 16811−16831.

(6) O'Keeffe, M.; Peskov, M. A.; Ramsden, S. J.; Yaghi, O. M. *Acc. Chem. Res.* **2008**, *41*, 1782−1789.

(7) Lehnert, R.; Seel, F. Z. *Z. Anorg. Allg. Chem.* **1980**, *464*, 187−194.

(8) Tian, Y. Q.; Zhao, Y. M.; Chen, Z. X.; Zhang, G. N.; Weng, L. H.; Zhao, D. Y. *Chem. - Eur. J.* **2007**, *13*, 4146−4154.

(9) Lanchas, M.; Vallejo-Sánchez, D.; Beobide, G.; Castillo, O.; Aguayo, A. T.; Luque, A.; Román, P. *Chem. Commun.* **2012**, *48*, 9930−9932.

(10) Karagiaridi, O.; Lalonde, M. B.; Bury, W.; Sarjeant, A. A.; Farha, O. K.; Hupp, J. T. *J. Am. Chem. Soc.* **2012**, *134*, 18790−18796.

(11) Shi, Q.; Kang, X.; Shi, F.; Dong, J. *Chem. Commun.* **2015**, *51*, 1131−1134.

(12) Crawford, D.; Casaban, J.; Haydon, R.; Giri, N.; McNally, T.; James, S. L. *Chem. Sci.* **2015**, *6*, 1645−1649.

(13) Banerjee, R.; Furukawa, H.; Britt, D.; Knobler, C.; O'Keeffe, M.; Yaghi, O. M. *J. Am. Chem. Soc.* **2009**, *131*, 3875−3877.

(14) (a) Tian, Y. Q.; Yao, S. Y.; Gu, D.; Cui, K. H.; Guo, D. W.; Zhang, G.; Chen, Z. X.; Zhao, D. Y. *Chem.—Eur. J.* **2010**, *16*, 1137−1141. (b) Karagiaridi, O.; Bury, W.; Sarjeant, A. A.; Stern, C. L.; Farha, O. K.; Hupp, J. T. *Chem. Sci.* **2012**, *3*, 3256−3260.

(15) (a) Empty **cag**-Zn(Im)$_2$ (ZIF-4) shows no N_2 uptake at low pressure (at 77 K), yet a BET surface area of 300 $m^2\ g^{-1}$. See: Bennett, T. D.; Cao, S.; Tan, J. C.; Keen, D. A.; Bithell, E. G.; Beldon, P. J.; Friščić, T.; Cheetham, A. K. *J. Am. Chem. Soc.* **2011**, *133*, 14546−14549. (b) **10mr**-Zn(Im)$_2$ exhibits a surface area of 319 m^2/g (ref 11).

(16) (a) Han, S. S.; Choi, S.; Goddard, W. A., III *J. Phys. Chem. C* **2010**, *114*, 12039−12047. (b) Battisti, A.; Taioli, S.; Garberoglio, G. *Microporous Mesoporous Mater.* **2011**, *143*, 46−53. (c) Keskin, S. *J. Phys. Chem. C* **2011**, *115*, 800−807. (d) Yilmaz, G.; Ozcan, A.; Keskin, S. *Mol. Simul.* **2015**, *41*, 713−726. (e) Guo, H.; Shi, F.; Ma, Z.; Liu, X. *J. Phys. Chem. C* **2010**, *114*, 12158−12165. Chen, E.; Liu, Y.; Zhou, M.; Zhang, L.; Wang, Q. *Chem. Eng. Sci.* **2012**, *71*, 178−184. (f) Wu, Y.; Chen, H.; Liu, D.; Qian, Y.; Xi, H. *Chem. Eng. Sci.* **2015**, *124*, 144−153. (g) Ding, L.; Yazaydin, A. O. *Phys. Chem. Chem. Phys.* **2013**, *15*, 11856−11861.

(17) (a) Nouar, F.; Eubank, J. F.; Bousquet, T.; Wojtas, L.; Zaworotko, M. J.; Eddaoudi, M. *J. Am. Chem. Soc.* **2008**, *130*, 1833−1835. (b) Guillerm, V.; Weseliński, Ł. J.; Belmabkhout, Y.; Cairns, A. J.; D'Elia, V.; Wojtas, Ł.; Adil, K.; Eddaoudi, M. *Nat. Chem.* **2014**, *6*, 673−680.

(18) Zhang, Z.; Zaworotko, M. J. *Chem. Soc. Rev.* **2014**, *43*, 5444−5455.

(19) Wang, B.; Côté, A. P.; Furukawa, H.; O'Keeffe, M.; Yaghi, O. M. *Nature* **2008**, *453*, 207−211.

(20) Beldon, P. J.; Fábián, L.; Stein, R. S.; Thirumurugan, A.; Cheetham, A. K.; Friščič, T. *Angew. Chem., Int. Ed.* **2010**, *49*, 9640−9643.

(21) (a) Ye, J. W.; Zhou, H. L.; Liu, S. Y.; Cheng, X. N.; Lin, R. B.; Qi, X. L.; Zhang, J. P.; Chen, X. M. *Chem. Mater.* **2015**, *27*, 8255−8260. (b) Morabito, J. V.; Chou, L.; Li, Z.; Manna, C. M.; Petroff, C. A.; Kyada, R. J.; Palomba, J. M.; Byers, J. A.; Tsung, C. *J. Am. Chem. Soc.* **2014**, *136*, 12540−12543.

(22) (a) Kane, C. M.; Banisafar, A.; Dougherty, T. P.; Barbour, L. J.; Holman, K. T. *J. Am. Chem. Soc.* **2016**, *138*, 4377−4392. (b) Kane, C. M.; Ugono, O.; Barbour, L. J.; Holman, K. T. *Chem. Mater.* **2015**, *27*, 7337−7354.

(23) (a) Joseph, A. I.; Lapidus, S. H.; Kane, C. M.; Holman, K. T. *Angew. Chem., Int. Ed.* **2015**, *54*, 1471−1475. (b) Joseph, A. I.; El-Ayle, G.; Boutin, C.; Léonce, E.; Berthault, P.; Holman, K. T. *Chem. Commun.* **2014**, *50*, 15905−15908.

(24) Lee, S.; Chen, C. H.; Flood, A. H. *Nat. Chem.* **2013**, *5*, 704−710.

(25) Holman, K. T.; Pivovar, A. M.; Ward, M. D. *Science* **2001**, *294*, 1907−1911.

(26) Zhang, J.; Wu, T.; Zhou, C.; Chen, S.; Feng, P.; Bu, X. *Angew. Chem., Int. Ed.* **2009**, *48*, 2542−2545.

DOI: 10.1021/jacs.6b06375
J. Am. Chem. Soc. 2016, 138, 12017−12020